ELSEVIER

Journal of Photochemistry and Photobiology A: Chemistry 102 (1996) 71–80

Journal of PHOTOCHEMISTRY AND PHOTOBIOLOGY A:CHEMISTRY

Factoring through-space and through-bond contributions to rates of photoinduced electron transfer in donor–spacer–acceptor molecules

David Gosztola [a], Bing Wang [a], Michael R. Wasielewski [a,b,*]

[a] *Chemistry Division, Argonne National Laboratory, Argonne, IL 60439-4831, USA*

[b] *Department of Chemistry, Northwestern University, Evanston, IL 60208-3113, USA*

Abstract

Contributions from direct orbital overlap (through-space interactions) and superexchange (through-bond interactions) to the electronic coupling matrix elements for photoinduced charge separation and recombination in a series of linked donor–spacer–acceptor molecules were studied. The molecules consisted of a 4-piperidinyl-naphthalene-1,8-dicarboximide (ANI) electron donor and a *N*-(n-octyl)pyromellitimide (PI) electron acceptor attached to the 1,5- and 1,8-positions of either anthracene (ANC) or dibenzobicyclo(2.2.2)octatriene (DBO) spacers. For the 1,8-disubstituted compounds, ANI and PI are held approximately cofacial with a center-to-center distance of 5.3 Å, whereas for the 1,5-disubstituted compounds, the center-to-center distance increases to 13.5 Å. The through-bond interaction was investigated by replacing the ANC spacer with DBO. The charge separation and recombination reactions were examined in both toluene and tetrahydrofuran (THF). The results show that for the 1,8-disubstituted DBO system in both toluene and THF, charge separation and recombination is dominated by through-space interactions. For the 1,8-disubstituted ANC system in both toluene and THF, charge separation occurs by means of a direct, through-space interaction, while charge recombination occurs through the intermediacy of the ANI–ANC$^+$–PI$^-$ ion pair in toluene and directly from ANI$^+$–ANC–PI$^-$ to ground state in THF. For the 1,5-disubstituted molecules, possessing either the ANC or the DBO spacers, electron transfer from ^{1}*ANI to PI was not kinetically competitive with the decay of ^{1}*ANI to ground state in either toluene or THF.

Keywords: Photoinduced electron transfer; Donor–spacer–acceptor molecules; Through-space interactions; Through-bond interactions

1. Introduction

It is well known that the rate of intramolecular electron transfer in linked donor–acceptor molecules is not only dependent upon the distance and orientation between the donor (D) and acceptor (A), but is also dependent upon the electronic properties of the intervening spacer (S) molecules between the redox centers [1–3]. If the distance between D and A is small enough to allow for direct overlap between the frontier orbitals of the donor and acceptor, electron transfer may occur by means of a through-space mechanism. When the D and A centers are too far apart for direct orbital overlap to be important, electron transfer may occur via a superexchange interaction. In order for superexchange to occur, there must be mixing of the D and A orbitals with the orbitals of the spacer molecule. The spacer molecule may consist of solvent [4], hydrogen-bonded bridging groups [5], salt bridges [6], or covalent bonds between the donor and acceptor [1–3]. When the intervening space between D and A is occupied primarily by chemical bonds, and the distance between D and A is large enough so that no direct orbital overlap occurs, then electron transfer occurs principally via through-bond interactions. In this paper, the terms through-space and through-bond are synonymous with direct overlap and superexchange, respectively. Both contributions to the total electronic coupling matrix element for electron transfer between the donor and acceptor depend on the distance and the orientation of the various molecular components. Thus, it is important to hold both the distance and geometry of the donor and acceptor fixed as the properties of the covalent spacer between them are varied. Achieving this degree of structural control in a D–S–A molecule is often a difficult task.

Previous studies of the distance dependence of photoinduced electron transfer have primarily utilized rigid, covalently-linked D–S–A molecules, where the D–S–A separation is so large as to obviate the through-space mechanism for electron transfer [7,8]. Very few studies of the through-space mechanism in the apparent absence of through-bond electron transfer exist because of the seemingly contradictory requirements of having the donor and acceptor in very close proximity, yet having the covalent linkage not give rise to

* Corresponding author.

1010-6030/96/$15.00 © 1996 Elsevier Science S.A. All rights reserved
PII S1010-6030(96)04365-1

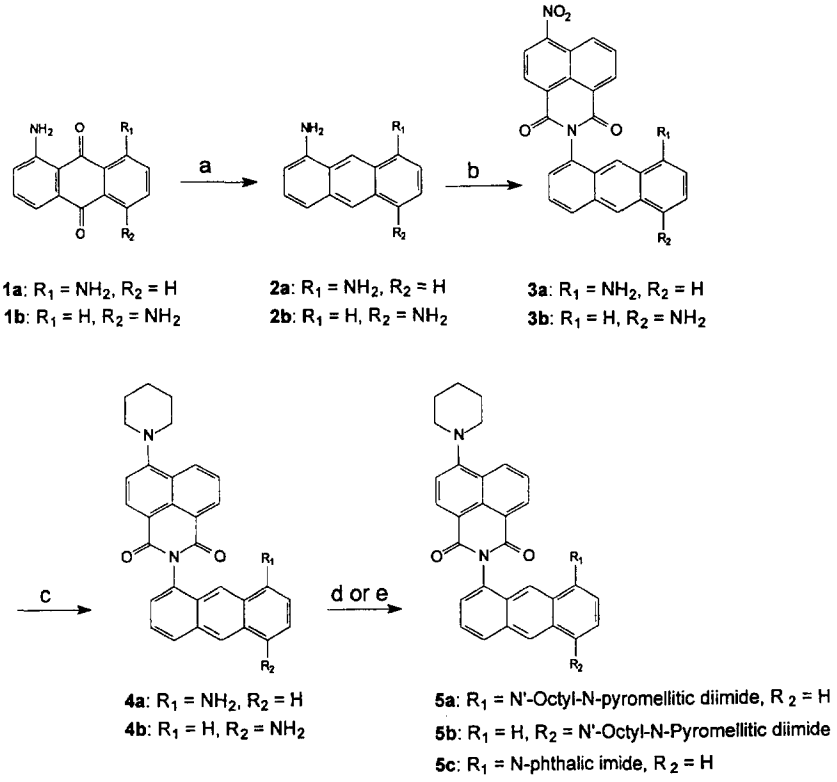

Scheme 1. Synthesis of anthracene spaced compounds. (a) $NaBH_4$, isopropanol, reflux, 24 h; (b) 4-nitro-1,8-naphthalic anhydride, EtOH, reflux, 17 h; (c) piperidene, DMF, reflux, 2h; (d) N-octyl-4,5-dicarboxyimidyl-1,2-phthalic anhydride, DMF, reflux, overnight; (e) phthalic anhydride, DMF, reflux, overnight.

through-bond electron transfer. Charge transfer complexes of aromatic molecules are specifically excluded from consideration here, because the donor and acceptor molecules within these complexes are free to adopt whatever minimum energy geometry is necessary to promote optimal charge transfer interaction within the complex. Some previous studies have utilized the "harpooning" mechanism to investigate through-space charge recombination [9–11] in polymethylene linked D–S–A molecules. The harpooning mechanism begins with a D–S–A molecule in an extended conformation in which photoinduced charge separation occurs via superexchange through the bonds of the polymethylene chain. After charge separation, electrostatic interactions between D^+ and A^- at the ends of the flexible spacer cause the spacer to fold, bringing D^+ and A^- into van der Waals contact and forming an exciplex-like state. Charge recombination can then occur via a through-space interaction. One limitation of these studies is that the charge recombination arises from a large ensemble of molecular orientations due to the multiplicity of folding geometries of the flexible polymethylene chain [9]. Rigid spacer groups offer much more control in fixing the donor–acceptor orientation and preventing their relative motion. Recently, Larson et al. have shown that energy transfer occurs in a series of covalently-linked, ruthenium-iron binuclear complexes where "the exchange process occurred without significant participation of the s-bonding linkage" [12].

In order to minimize the through-bond contribution to electron transfer for a bridging system capable of holding a donor–acceptor couple close enough for through-space interactions, we need to do the opposite of what is known to be necessary to enhance through-bond electron transfer [7]. We need saturated, rigid bonds between the donor and acceptor with numerous cis linkages. In a previous paper, we used a calix[4]arene moiety in its cone conformation to hold a donor–acceptor molecule close to a carotenoid molecule in order to probe the electric field generated from photoinduced charge separation [13]. Experiments carried out at that time showed that when the porphyrin donor and pyromellitimide acceptor were attached to the 5 and 17 positions, respectively, of the calix[4]arene spacer with a through-space distance of about 7 Å, no electron transfer was detectable. Thus, a spacer with a long, through-bond pathway similar to that of the calix[4]arene is required to inhibit through-bond electron transfer, and at the same time position D and A close to one another. In this paper we present a study of a series of linked D–S–A molecules based on 1,8- and 1,5-disubstituted anthracene (ANC) and dibenzobicyclo(2.2.2.)octatriene (DBO) spacers. These spacers position the ANI donor and PI acceptor at fixed distances relative to one another, provide the desired rigidity, and strongly limit through-bond electron transfer.

2. Results

2.1. Synthesis

Anthracene has been used previously as a rigid spacer group for cofacial porphyrins in a number of studies begin-

ning with Chang and Abdalmudhi in 1983 [14]. These types of molecules have been used to study catalytic redox chemistry [15], O_2 binding [16], and as models for the photosynthetic reaction center [17]. The synthesis of the anthracene spaced compounds is shown in Scheme 1. Compounds **5a** and **5b** were further reacted via Scheme 2 to break the aromaticity of the anthracene spacer by converting it into dibenzobicyclo(2.2.2)octatriene (DBO) (**6a** and **6b**).

2.2. Spectroscopy

The ground state absorption spectra of compounds **5a** and **6a** in toluene are shown in Fig. 1. Both spectra display the 400 nm charge transfer absorption band of ANI. The spectrum of **5a** also shows structured absorption bands at wavelengths below 400 nm that are characteristic of the anthracene spacer. The spectra of **6a** and **6b** are indistinguishable from reference molecule **7** (Scheme 3) [18]. The ANI absorption bands in the spectra of **5a** and **5b** are the same as in reference molecule **5c**, although the anthracene bands are less well resolved in **5b**. Similar spectra were observed in THF. Fluorescence quantum yields (ϕ_f) determined in toluene and THF are listed in Table 1. The fluorescence arises from the excited CT state of the ANI chromophore, which has a fluorescence quantum yield of 0.91 in toluene [18]. The fluorescence emission from **5a** and **6a** is strongly quenched in both toluene and THF,

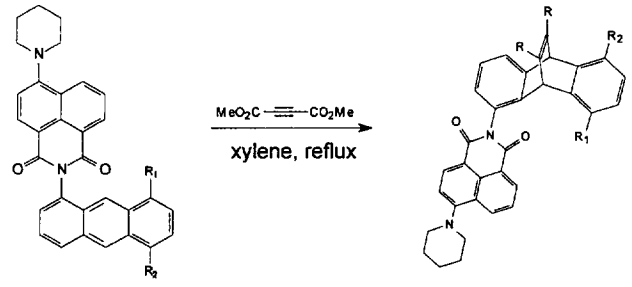

Scheme 2. Reaction of **5a** and **5b**.

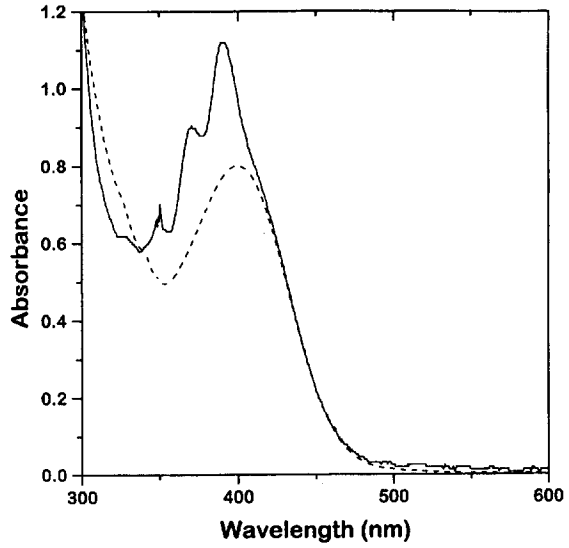

Fig. 1. Ground state absorption spectra of **5a** (———) and **6a** (——) in toluene.

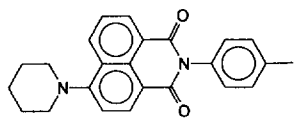

7

Scheme 3. Compound **7**.

Table 1
Fluorescence quantum yield, Φ_f, charge separation time constant, τ_{cs}, and charge recombination time constant, τ_{cr}, for selected compounds

Compound	Solvent	Φ_f	τ_{cs} (ps)	τ_{cr} (ps)
7	Toluene	0.91	–	8500
5a	Toluene	<0.001	0.45	70, 250
5b	Toluene	0.90	>8500	–
6a	Toluene	0.007	0.45	430
6b	Toluene	0.90	>8500	–
7	THF	0.72	–	8500
5a	THF	<0.001	0.46	39
5b	THF	0.70	>8500	–
6a	THF	<0.001	0.48	43
6b	THF	0.70	>8500	–

whereas **5b** and **6b** exhibit very little quenching in either solvent.

Cyclic voltammetry was used to measure the single electron oxidation and reduction potentials of the various molecules for use in driving force calculations (vide infra). Table 2 lists the half-wave potentials as well as whether the redox chemistry was donor, acceptor, or bridge based.

The transient absorption spectrum of **6a** in toluene recorded 20 ps after 412 nm excitation is shown in Fig. 2. This spectrum shows the characteristic transient absorption bands of PI^- at 655 nm and 715 nm [17]. The presence of the 715 nm band is conclusive evidence that photoinduced electron transfer has occurred. The band at 475 nm is a less useful diagnostic because it is composed of absorption due to both ^{1}*ANI and ANI^+. The formation and decay kinetics for PI^- in molecule **6a** were monitored at 715 nm and are shown in Fig. 3. This data can be fit with a single exponential rise and decay. The time constant for charge separation is 0.45 ps and the time constant for charge recombination is 430 ps. When monitored at 460 nm (not shown), the rise time was instrument limited due to the nearly instantaneous formation of ^{1}*ANI. The decay time of the 460 nm band was 440 ps, which is in good agreement with the decay time of PI^-. Similar measurements were made for **5a**. The transient

Table 2
Electrochemical oxidation and reduction potentials for selected compounds in butyronitrile/0.1 M tetra-n-butylammonium perchlorate. All potentials are half-wave versus SCE

Compound	E_{OX} donor	E_{RED} acceptor	E_{OX} bridge	E_{RED} bridge
5a	1.26	−0.79	1.58	−2.13
5c	1.19		1.40	−2.02
6c	1.18		>1.85	−1.76

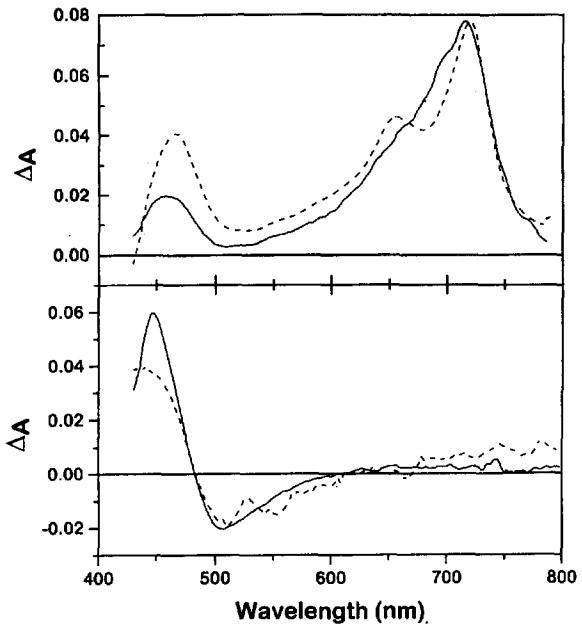

Fig. 2. Top: transient absorption spectra of **5a** (———) and **6a** (——) in toluene 20 ps after excitation with a 140 fs pulse at 412 nm. Bottom: transient absorption spectra of **5b** (———) and **6b** (——) in toluene 20 ps after excitation with a 140 fs pulse at 412 nm.

absorption spectrum of **5a** (Fig. 2, top) also shows the intense 715 nm band, which indicates that charge transfer has occurred. However, the 655 nm band appears as a shoulder probably due to spectral overlap with another absorption band. Kinetic arguments presented below suggest that this band may belong to the anthracene radical cation, which appears as an intermediate in the charge recombination reaction within **5a**. Monitoring the formation and decay kinetics of **5a** at 715 nm (Fig. 3) gives a charge separation time constant of 0.45 ps and a biexponential charge recombination time constant of 70 ps and 250 ps with the faster component making up 65% of the total amplitude. Fig. 4 shows the transient absorption kinetics for the formation and decay of PI^-

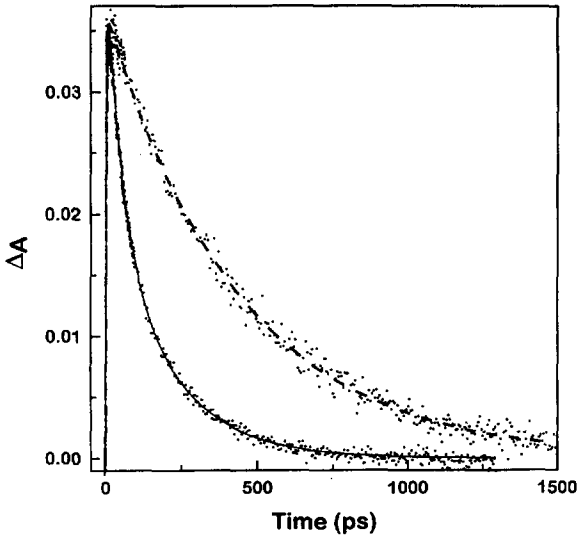

Fig. 3. Transient absorption kinetics of **5a** (———) and **6a** (——) in toluene monitored at 715 nm following a 140 fs pulse at 412 nm.

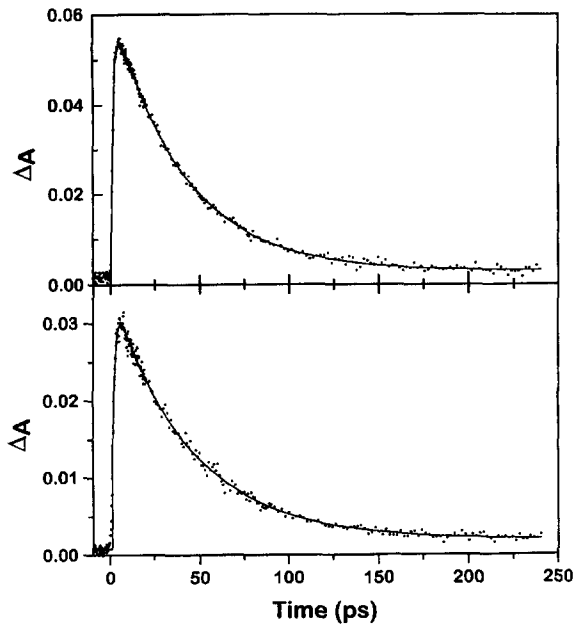

Fig. 4. Transient absorption kinetics of **5a** (top) and **6a** (bottom) in THF monitored at 715 nm following a 140 fs pulse at 412 nm.

in **5a** and **6a** in THF monitored at 715 nm. In the higher polarity solvent the time constants for the decay of $ANI^+ - PI^-$ decreases (Table 1). Unlike the result obtained for **5a** in toluene, the decay of PI^- within **5a** in THF is fit adequately with a single exponential decay time.

A second set of molecules, **5b** and **6b**, in which the center-to-center distance between ANI and PI increases to 13.5 Å, but the through-bond pathway only increases by one bond, showed no evidence for PI^- formation when monitored at 715 nm. Fig. 2, bottom, shows the transient absorption spectra of both **6b** and **5b** showing that only ^{1}*ANI is present.

3. Discussion

Accurate determinations of the energy levels of ion pair states in donor–acceptor molecules in low polarity media are difficult. Frequently, the CT or ion pair states produced by photochemical charge separation recombine non-radiatively to their ground states. Thus, direct spectroscopic information about the energy levels of the charge separated states is not available. In polar media the sum of the thermodynamic potentials for oxidation of the donor and reduction of the acceptor often give a reasonable estimate of the ion pair state energy. However, for low polarity media one must resort to modeling the change in solvation energy of the ions that occurs when the ions are taken from a medium with a high static dielectric constant to one that is low. Weller developed an expression based on the Born dielectric continuum model of the solvent to determine the ΔG of formation for an ion pair in a solvent of arbitrary polarity [19]:

$$\Delta G = E_{OX} + E_{RED} - \frac{e^2}{r_{12}\epsilon_s} + e^2\left(\frac{1}{2r_1} + \frac{1}{2r_2}\right)\left(\frac{1}{\epsilon_s} - \frac{1}{\epsilon_p}\right) \quad (1)$$

where E_{OX} and E_{RED} are, respectively, the oxidation and reduction potentials of the donor and acceptor in a high polarity solvent with static dielectric constant ϵ_p, e is the charge of the electron, r_{12} is the ion pair distance, r_1 and r_2 are the ionic radii, and ϵ_s is the static dielectric constant of the low polarity solvent. The term involving the ion pair distance is simply the coulombic interaction of the ions. The last term accounts for the ability of lower polarity solvents to weakly stabilize charges as compared to the high polarity solvent used in the electrochemical measurements. It is well known that Eq. (1) overestimates the degree of destabilization of an ion pair in low polarity solvents relative to those with high polarity [20].

Direct spectroscopic measurements of the ion pair state energies, ΔG, and the total reorganization energy for the charge transfer, λ, are possible using Eqs. (2) and (3), if these states undergo radiative recombination, and the potential surfaces for each state are similar in shape [21].

$$\Delta G = \frac{E_a + E_e}{2} \tag{2}$$

$$\lambda = \frac{E_a - E_e}{2} \tag{3}$$

Using Eqs. 2 and 3, we determined previously that the excited CT state energy of ANI is 2.80 eV [18]. In addition, the total reorganization energy, λ for formation of the ANI CT state is 0.3 eV. The total reorganization energy $\lambda = \lambda_I + \lambda_s$, where λ_I is the reorganization energy due to the internal modes of the molecule, and λ_s is due to the reorganization of the solvent. Marcus has shown that

$$\lambda_s = e^2\left(\frac{1}{2r_1} + \frac{1}{2r_2} - \frac{1}{r_{12}}\right)\left(\frac{1}{\epsilon_o} - \frac{1}{\epsilon_s}\right) \tag{4}$$

where e, r_{12}, r_1, r_2, and ϵ_s are defined above, and ϵ_o is the high frequency dielectric constant of the solvent [22]. For toluene, $\epsilon_o \cong \epsilon_s$, so that Eq. (4) yields $\lambda_s \cong 0$. Thus, $\lambda_I = 0.3$ for ANI. Since this value is typical of organic π donors and acceptors [23], we assume that a similar value of λ_I is valid for electron transfer reactions involving molecules of similar structural type, such as **5a**, **5b**, **6a** and **6b**.

The electron transfer reactions from ^{1}*ANI to PI are essentially charge shift reactions because ^{1}*ANI is strongly CT in nature with 70% charge transfer character [18]. The free energies of the charge shift reactions within **5a**, **5b**, **6a** and **6b** can be determined by taking into account the change in redox potential for reduction of PI versus ANI and the change in Coulomb energy needed to separate the charges the additional distance. As an approximation we will assume that a large fraction of the energy change required to solvate the charges of the ion pair is already included in the spectroscopically determined energy of the initial ANI CT state. Thus, the energies of the fully charge separated states in the ANI–spacer–PI molecules are given by:

$$\Delta G_{IP2} = \Delta G_{IP1} + E_{RED}(\text{ANI}) - E_{RED}(\text{PI}) + \frac{e^2}{\epsilon_s}\left(\frac{4.8\,q^3}{\mu} - \frac{1}{r_{IP2}}\right) \tag{5}$$

where ΔG_{IP1} and ΔG_{IP2} are the free energies of formation of the initial ^{1}*ANI CT state and the $ANI^+ - PI^-$ ion pair state, respectively, $E_{RED}(\text{ANI})$ and $E_{RED}(\text{PI})$ are the potentials for reduction of ANI and PI, respectively, r_{IP2} is the ion pair distance in $ANI^+ - PI^-$, q is the fractional degree of charge separation within ^{1}*ANI, and μ is the excited state dipole moment of ^{1}*ANI. Eq. (5) assumes that $E_{RED}(\text{ANI}) - E_{RED}(\text{PI})$ is the same in toluene and PrCN [18]. The value r_{IP2} was determined from energy minimized structures of the dyads using force-field calculations (molecular structure parameters were determined from an MM2 energy-minimized structure using Hyperchem software [24]), while the value of μ was determined to be 11.1 D from solvatochromic changes of the emission spectrum of ^{1}*ANI [18,25]. The solvent dielectric constants are from Ref. [26]. The energies of **5a**, **5b**, **6a** and **6b** in toluene and THF determined from Eq. (5) are given in Table 3 along with the values calculated using the method of Weller (Eq. (1)). For the Weller calculation ionic radii of 3.5 Å were used. The data in Table 3 show that the Weller method consistently overestimates the energies of the ion pair states by about 0.5 eV in toluene.

We can use the values of ΔG for both charge separation and recombination from Table 3 along with estimates of λ_s calculated from Eq. (4), $\lambda_I = 0.3$ eV, and the experimentally determined rate constants, k_{CT} to determine the electronic coupling matrix element, V for the electron transfer reactions using the standard expression from semi-classical electron transfer theory [27–29],

$$k_{CT} = \frac{V_{DA}^2}{\hbar}\sqrt{\pi/\lambda_s k_B T}\sum_{j=0}^{\infty}\exp(-S)\frac{S^j}{j!} \exp\left(-\frac{(\Delta G + \lambda_s + j\hbar\omega)^2}{4\lambda_s k_B T}\right) \tag{6}$$

where ω is the vibrational quantum, usually assumed to be 1 500 cm^{-1} and $S = \lambda_i/\hbar\omega$. The summation j is done over the quantum number of the high frequency vibrational modes in the radical pair state. The values of V predicted for charge separation and recombination in **5a** and **6a** in both toluene and THF are given in Table 4. In toluene the electronic cou-

Table 3
Energy levels for the ion pair intermediates.

Compound	Solvent	ΔG (Eq. (5))	ΔG (Eq. (1))
5a, 6a	Toluene	1.91	2.33
5b, 6b	Toluene	2.60	3.03
5a, 6a	THF	2.04	1.95
5b, 6b	THF	2.28	2.19

Table 4
Electronic coupling matrix elements for **5a** and **6a**

Solvent	V_{CS} (cm^{-1})	V_{CR} (cm^{-1})
Toluene	207	510
THF	67	202

pling matrix elements for charge recombination in **5a** and **6a** are about 2.5 times larger than those for charge separation. In addition, the values of V for both charge transfer reactions in **5a** and **6a** in toluene are about 2.5–3 times larger than those estimated from data obtained in THF.

The electronic coupling matrix element, V can be broken down into component parts related to the direct donor–acceptor orbital overlap [30], V_D, indirect orbital overlap through intervening bonds, V_I, and indirect overlap through non-bonding interactions such as intervening solvent molecules, V_{IS}. The total electronic coupling can be expanded as the sum of these different interactions:

$$V = V_D + V_I + V_{IS} \quad (7)$$

The terms V_D and V_{IS}, are not easily separated, because these experiments were carried out in a condensed phase. However, since toluene and THF do not have low-lying orbitals that can accept an electron or hole, no direct hopping mechanism can be seriously considered for electron transfer in these media. Likewise, a through-solvent superexchange mechanism is likely to make a minor contribution to the total V, because there are no covalent linkages between donor, acceptor, and the individual solvent molecules. Therefore, the contribution from V_{IS}, will be neglected in this analysis.

Comparing the two 1,8-disubstituted molecules, **5a** and **6a**, the through-bond interaction, V_I, involves six bonds between the imide nitrogen atom of ANI and that of PI. Changing the nature of the bonding network from two saturated bonds in **5a** to four saturated bonds in **6a** does not change the overall rate constant for electron transfer to PI. Despite the fact that the systems of both ANI and PI are not coplanar with the corresponding planes of the anthracene in **5a** and of the phenyl rings in **6a** [24], some mixing of the anthracene orbitals with those of ANI and PI may be important. The fact that the total V, as directly determined from the rate constants for charge separation within **5a** and **6a**, remains constant, suggests that the V_I term in Eq. (7) is either constant or unimportant relative to V_D. If we then compare the results for the 1,8-disubstituted molecules with the corresponding 1,5-disubstituted compounds, the 1,5 donor–acceptor systems have only one additional bond between the donor and acceptor than the 1,8 systems. While the center-to-center (through-space) distances between ANI and PI in **5a** and **6a** are 5.3 Å, the corresponding through-bond distances are 9.0 Å. Similarly, while the center-to-center (through-space) distances in **5b** and **6b** are 13.5 Å, the corresponding through-bond distances are 10.5 Å. Thus, the direct orbital overlap term, V_D should be large in **5a** and **6a** and very small in **5b** and **6b** while the through-bond term, V_I should be similar in all of these molecules.

Even though no electron transfer from the ANI CT state to PI was observed in both **5b** and **6b**, we can predict the rate constant for the formation of ANI^+–PI^- in these molecules using the corresponding measured rate constants for **5a** and **6a**, along with the assumption that all the rate constants are determined by the indirect, through-bond term, V_I, alone. Electron transfer rates have been shown to decay exponentially as the distance between the donor and acceptor increases [7,8,23]:

$$k = k_0 e^{-\beta(r - r_0)} \quad (8)$$

where k_0 is the rate constant at distance r_0, r is the distance between D and A and β is a parameter that is typically about 1.0 $Å^{-1}$ for through-bond interactions and 2–3 $Å^{-1}$ for through-space interactions. For this analysis we assume that the total electronic coupling matrix element $V = V_I$, i.e. through-bond coupling is the only contribution to the coupling between D and A. The value of r_0 is obtained from the through-bond distance between ANI and PI and k_0 is the rate constant for formation of ANI^+–PI^- in **5a** and **6a**. Eq. (8) predicts that the rate constants for charge separation within **5b** and **6b** with $r_0 = 9$ Å and $r = 10.5$ Å should be 5.0×10^{11} s^{-1} for $k_0 = 2.2 \times 10^{12}$ s^{-1} (toluene), and 4.8×10^{11} s^{-1} for $k_0 = 2.1 \times 10^{12}$ s^{-1} (THF). Since no ANI^+–PI^- is formed competitively with the decay of ^{1}*ANI, electron transfer from ^{1}*ANI to PI in **5b** and **6b** is substantially slower than the intrinsic 2×10^8 s^{-1} decay rate of ^{1}*ANI. Thus, the rate constants predicted for **5b** and **6b** using Eq. (8) are at least three orders of magnitude too large. This analysis suggests that our original assumption concerning the dominance of the V_I term in the total electronic coupling is incorrect, and in fact, V_I is small for electron transfer in **5a** and **6a**, as well as in **5b** and **6b**. There are at least two possible reasons for this behavior. First, as mentioned above, the orientation of the π systems of the donor and acceptor are twisted relative to the π systems of the bridges. This should diminish orbital overlap, thus reducing the electronic coupling. Second, the through-bond pathway is a mixture of cis and trans bond orientations, and in the case of **6a** and **6b**, a mix of σ and π bonds. These conditions combine to give a very weak electronic coupling through the two types of bridges used here.

While the charge recombination kinetics in **6a** can be described adequately by a single exponential decay, the charge recombination kinetics in **5a** were found to be biexponential. Table 2 shows that the anthracene bridge in **5a** and **5b** undergoes oxidation at a potential that is 0.2–0.3 V more positive than that of ANI. The energy of a hypothetical ion pair state with a positive charge on the anthracene bridge can be calculated from:

$$\Delta G_{IP2} = \Delta G_{IP1} - E_{OX}(\mathrm{ANI}) + E_{OX}(\mathrm{ANC}) - \frac{e^2}{\epsilon_s}\left(\frac{1}{r_{IP2}} - \frac{1}{r_{IP1}}\right) \quad (9)$$

where the terms are defined as in Eq. (5). With $r_{IP1} = 5.3$ Å and $r_{IP2} = 4.0$ Å, Eq. (9) yields a 1.87 eV energy for the ANI–ANC^+–PI^- ion pair in toluene. This is 40 mV lower than the energy of the ANI^+–ANC–PI^- ion pair state. It is therefore likely that the charge recombination proceeds via the ANI–ANC^+–PI^- ion pair state intermediate. The 250 ps component in the charge recombination reaction for **5a** can be identified with the reaction ANI^+–Anth–PI^- → ANI–

$Anth^+$–PI^-, while the 70 ps component is most likely due to the reaction ANI–$Anth^+$–PI^- → ANI–Anth–PI. As mentioned earlier, the anthracene radical cation may be contributing to the broadening of the transient absorption spectrum of **5a** in toluene shown in Fig. 2 [31]. Convolution of the ANC^+ band with that of PI^- makes it difficult to measure kinetics for ANC^+ alone. Eq. (9) yields a 2.24 eV energy for the ANI–ANC^+–PI^- ion pair in THF. Thus, the energy of this intermediate is about 0.2 eV above that of ANI^+–ANC–PI^- in THF precluding participation of the ANI–ANC^+–PI^- ion pair as an intermediate along the pathway for charge recombination. This is consistent with the fact that the decay of ANI^+–ANC–PI^- to ground state in THF is adequately described by a single exponential time constant. No intermediary charge recombination step involving the spacer is observed for **6a**, because the DBO bridge cannot be easily oxidized or reduced within **6a**.

4. Conclusions

The results given in this paper show that charge separation within the 1,8-disubstituted ANI–DBO–PI and ANI–ANC–PI molecules is most likely dominated by through-space interactions. Charge recombination within ANI^+–DBO–PI^- proceeds by a single-step mechanism, once again most likely via a through space interaction. On the other hand, charge recombination within ANI^+–ANC–PI^- proceeds via the ANI–ANC^+–PI^- intermediate in toluene and occurs with no observable intermediate in THF. Charge separation does not occur in the corresponding 1,5-disubstituted compounds at a rate that is competitive with the decay of ^{1}*ANI. These results show that it is possible to use a circuitous bonding pathway to decrease the electronic coupling matrix element in a donor–spacer–acceptor molecule to such an extent that the direct orbital overlap contribution to the total electronic coupling matrix element can dominate. These results have implications in the design of complex donor–acceptor molecules in which the donor and acceptor must be held at close, fixed distances with little or no through-bond interaction. This has particular relevance for donor–spacer–acceptor molecules designed to study the influence of solvent between a donor and an acceptor on electron transfer rates.

5. Experimental

All solvents and reagents were reagent grade quality and used as received. Solvents for all spectroscopic measurements were dried over 3 Å molecular sieves. All spectroscopic samples were contained in sealed 1 mm cuvettes and deaerated with nitrogen prior to use. Thin layer chromatography (TLC) was performed on commercially prepared silica gel plates purchased from ES Science. Column chromatography was performed using Merck silica gel 60 as the solid support.

6. Spectroscopy

Proton nuclear magnetic resonance (^{1}H NMR) was recorded on a General Electric GE-300 NMR spectrometer using tetramethylsilane (TMS) as internal standard. Ground state UV-vis spectra were recorded using a Shimadzu model UV-160 spectrophotometer. Laser desorption mass spectra were obtained with a Kratos MALDI III spectrometer. Fluorescence measurements were made with a Photonics Technologies International model QMI fluorimeter. Relative quantum yields were determined using 9,10-diphenylanthracene, $\phi = 0.90$ [32], and ANI, ($\varphi = 0.91$)[18], as references. Electrochemical measurements were made using a Princeton Applied Research model 273 potentiostat, a Pt working electrode and a $Ag/AgNO_3$ reference electrode. Ferrocene was used to determine the potential offset versus SCE.

The femtosecond transient absorption system has been previously described [13,18,33]. Briefly, the amplified output of a Ti:sapphire laser (300 μJ, 824 nm) was split and 95% was frequency doubled to serve as the pump beam. Samples were typically excited with 2–3 μJ, 150 fs, 412 nm pulses. The remaining 5% of the amplified 824 nm light was used to generate a white light continuum probe by focusing into a piece of slowly rotating fused silica. Amplified photodiodes were used to detect single wavelengths of the probe light after it passed through a monochromator (SPEX model 270M). The photodiode outputs were digitized and recorded using a personal computer. Multiexponential rise and decays to the data were determined using the Levenberg–Marquardt algorithm.

6.1. Synthesis

6.1.1. 1,8-Diaminoanthracene (2a) [34]

A solution of 1,8-diaminoanthraquinone[35] (2.0 g, 8.4 mmol) in isopropanol (100 ml) was bubbled with nitrogen for 15 min before the introduction of sodium borohydride (4.0 g, 106 mmol). The resulting suspention was heated at reflux under nitrogen atmosphere for 60 h. After cooling to room temperature, the reaction mixture was poured into ice water (250 ml). The dark precipitates were filtered off, washed thoroughly with water and then dissolved in chloroform (100 ml). The resulting solution was dried over anhydrous sodium sulfate before being concentrated on a rotary evaporator under reduced pressure. Purification was then carried out a silica gel column using 0–3% methanol in chloroform as the eluents. This gave 1.0 g of product **2a** as a dark solid (57.0%). ^{1}H NMR ($CDCl_3$) δ 3.83 (s, br, 4H, NH_2), 6.76 (d, $J = 7.8$ Hz, 2H, H2 and H7), 7.30 (t, 2H, $J' = 7.5$ Hz, $J'' = 8.4$ Hz, H3 and H6), 7.48 (d, 2H, $J = 8.3$ Hz, H4 and H5), 8.35 (s, 1H, H10), 8.37 (s, 1H, H9). Mass spectrum *m/e*: calcd., 208.3; found, 208.5.

6.1.2. 1,5-Diaminoanthracene (2b)

A solution of 1,5-diaminoanthraquinone (3.0 g, 12.6 mmol) in isopropanol (150 ml) was bubbled with nitrogen for 15 min before the introduction of sodium borohydride

(6.0 g, 159 mmol). The resulting suspension was heated at reflux under nitrogen atmosphere for 48 h and then cooled in a refrigerator for 2 h. The dark brown precipitates were filtered off and washed carefully with acetone. The resulting greenish solution was passed through a short silica gel column using acetone as the eluent, giving a brown solution. Evaporation of solvent on a rotary evaporator afforded ca. 3.0 g dark brown syrup which was unstable, and therefore, was used for next step without further purification. Mass spectrum *m/e*: calcd., 208.3; found, 208.1.

6.1.3. 1-Amino-8-(4-nitro-1,8-naphthalic imidyl) anthracene (3a)

A solution of **2a** (0.73 g, 3.5 mmol) and 4-nitro-1,8-naphthalic anhydride (0.85 g, 3.5 mmol) in absolute ethanol (50 ml) was refluxed overnight. The black solid was filtered off after the reaction mixture was cooled to room temperature. Being washed with ethanol and air dried, the obtained solid was then dissolved in a small amount of chloroform. This solution was loaded onto the top of a silica column and eluted with 1% MeOH in $CHCl_3$. This furnished product **3a** (0.20 g, 13.2% yield). ^{1}H NMR ($CDCl_3$) δ 3.99 (s, br, 2H, NH_2), 6.70 (d, J = 7.71 Hz, 1H, anthralic H2), 7.30 (t, 1H, J' = 7.28 Hz, J'' = 7.28 Hz, anthralic H3), 7.46 (d, 1H, J = 6.86 Hz, anthralic H4), 7.51 (d, 1H, J = 8.14 Hz, anthralic H5), 7.58 (t, 1H, J' = 8.14 Hz, J'' = 8.56 Hz, anthralic H6), 8.03 (t, 1H, J' = 7.28 Hz, J'' = 7.29 Hz, naphthalic H'6), 8.09 (s, 1H, H10), 8.16 (d, 1H, J = 8.56 Hz, anthralic H7), 8.35 (s, 1H, anthralic H10), 8.48 (d, 1H, J = 8.13 Hz, naphthalic H'2), 8.53 (s, 1H, anthralic H9), 8.76 (d, 1H, J = 8.14 Hz, naphthalic H'3), 8.82 (d, 1H, J = 7.28 Hz, naphthalic H'5), 8.93 (d, 1H, J = 7.71 Hz, naphthalic H'7). Mass spectrum *m/e*: calcd., 433.4; found, 433.0.

6.1.4. 1-Amino-5-(4-nitro-1,8-naphthalic imidyl) anthracene (3b)

This compound was made from crude **2b** (1.2 g, 5.7 mmol) and 4-nitro-1,8-naphthalic anhydride (0.70 g, 2.9 mmol) in a similar manner as described in the preparation of **3a**. Yield 10.0%. ^{1}H NMR ($CDCl_3$) δ 4.00 (s, br, 4H, NH_2), 6.76 (d, J = 7.8 Hz, 2H, H2 and H7), 7.30 (t, 2H, J' = 7.5 Hz, J'' = 8,4 Hz, H3 and H6), 7.48 (d, 2H, J = 8.3 Hz, H4 and H5), 8.35 (s, 1H, H10), 8.37 (s, 1H, H9). Mass spectrum *m/e*: calcd., 433.4; found, 433.3.

6.1.5. 1-Amino-8-(4-piperidyl-1,8-naphthalic imidyl) anthracene (4a)

A solution of **3a** (0.19 g, 0.4 mmol) and piperidine (2.0 ml) in *N,N*-dimethyl formamide (DMF) (10 ml) was brought to reflux for 4 h. The reaction mixture was allowed to cool to room temperature and then poured into water. The precipitates were collected by filtration, subsequently dissolved in chloroform, and dried over anhydrous sodium sulfate. After concentration on a rotary evaporator under reduced pressure, the solution was transferred onto the top of a silica gel column. Eluting with 3% acetone in chloroform yielded 70 mg **4a** (37.1%). ^{1}H NMR ($CDCl_3$) δ 1.76 (m, 2H, CH_2), 1.92 (m, 4H, CH_2), 3.30 (m, 4H, NCH_2), 3.97 (br. s, 2H, NH_2), 6.65 (d, 1H, J = 6.43 Hz, anthralic H2), 7.21–7.25 (t + d, 2H, anthralic H3, and naphthalic H'2), 7.45 (d, 1H, J = 6.86 Hz, anthralic H5), 7.47 (d, 1H, J = 8.57 Hz, anthralic H4), 7.57 (t, 1H, J' = 8.57 Hz, J'' = 8.14 Hz, anthralic H6), 7.75 (t, 1H, J' = 8.13 Hz, J'' = 7.29 Hz, naphthalic H'6), 8.12 (d, 1H, J = 8.56 Hz, anthralic H7), 8.13 (s, 1H, anthralic H10), 8.48 (s, 1H, anthralic H9), 8.49 (d, 1H, J = 8.56 Hz, naphthalic H'5), 8.56 (d, 1H, J = 8.14 Hz, naphthalic H'2), 8.63 (d, 1H, J = 7.28 Hz, naphthalic H'7). Mass spectrum *m/e*: calcd., 471.6; found, 471.6.

6.1.6. 1-Amino-5-(4-piperidyl-1,8-naphthalic imidyl) anthracene (4b)

This compound was made from **3b** (40 mg, 0.07 mmol) and piperidine (1.0 ml) using a similar procedure for the preparation of **4a**. Yield 93.4%. ^{1}H NMR ($CDCl_3$) δ 1.77 (m, 2H, CH_2), 1.94 (m, 4H, CH_2), 3.32 (m, 4H, NCH_2), 4.30 (br. s, 2H, NH_2), 6.69 (d, 1H, J = 6.86 Hz, anthralic H2), 7.17 (t, 1H, J' = J'' = 7.28 Hz, anthralic H3), 7.22–7.27 (m, 2H, anthralic H4, and naphthalic H'3), 7.48 (d, 1H, J = 6.85 Hz, anthralic H8), 7.57 (t, 1H, J' = 6.57 Hz, J'' = 8.14 Hz, anthralic H7), 7.76 (t, 1H, J' = 8.14 Hz, J'' = 8.57 Hz, naphthalic H'6), 8.11 (s, 1H, anthralic H10), 8.12 (d, 1H, J = 7.73 Hz, anthralic H6), 8.49 (s, 1H, anthralic H9), 8.51 (d, 1H, J = 8.57 Hz, naphthalic H'5), 8.60 (d, 1H, J = 8.14 Hz, naphthalic H'2), 8.66 (d, 1H, J = 7.23 Hz, naphthalic H'7). Mass spectrum *m/e*: calcd., 471.6; found, 471.8.

6.1.7. 1-(N'-Octyl-1,2,4,5-benzene diimide-N-yl)-8-(4-piperidyl-1,8-naphthalic imidyl) anthracene (5a)

A solution of **4a** (60 mg, 0.13 mmol) and *N*-octyl-4,5-imidyl-1,2-phthalic anhydride (100 mg, 0.30 mmol) in DMF (10 ml) was heated at reflux for 23 h. The solvent was then removed under reduced pressure. The resulting residue was purified by column chromatography on silica gel using 1% acetone in dichloromethane as the eluent. Product **5a** was obtained as a yellow solid (63 mg, 61.9%). ^{1}H NMR ($CDCl_3$) δ 0.91 (t, 3H, $CH_2(CH_2)_6CH_3$), 1.25–1.40 (m, 10H, $CH_2CH_2(CH_2)_5CH_3$), 1.76 (m, 4H, piperidyl H'''4, and $CH_2CH_2(CH_2)_5CH_3$), 1.92 (m, 4H, piperidyl H'''3 and H'5), 3.15 (m, 4H, piperidyl H'''2 and H'''6), 3.96 (m, 2H, $CH_2CH_2(CH_2)_5CH_3$), 7.20 (d + t, 2H, naphthalic H'3 and anthralic H3), 7.46–7.64 (m, 6H, anthralic H2, H4, H5, H6, H7, and naphthalic H'6), 7.66 (s, 1H, anthralic H10), 8.15–8.20 (m, 3H, naphthalic H'5, and pyromellitic H''3, H''6), 8.49 (d, 2H, naphthalic H'2 and H'7), 8.67 (s, 1H, anthralic H9). Mass spectrum *m/e*: calcd., 782.9; found, 781.7.

6.1.8. 1-(N'-Octyl-1,2,4,5-benzene diimide-N-yl)-5-(4-piperidyl-1,8-naphthalic imidyl) anthracene (5b)

This compound was made from **4b** (100 mg, 0.20 mmol) and *N*-octyl-4,5-imidyl-1,2-phthalic anhydride (410 mg, 1.2 mmol) using a similar procedure for preparation of **5a**. Yield 28.1%. Mass spectrum *m/e*: calcd., 782.9; found, 782.5.

6.1.9. 1-(Phthalic imidyl)-8-(4-piperidyl-1,8-naphthalic imidyl)anthracene (5c)

This compound was made from **4a** (17 mg, 0.036 mmol) and phthalic anhydride (100 mg, 1.2 mmol) using a similar procedure for preparation of **5a**. Yield 90.0%. ^{1}H NMR ($CDCl_3$) δ 1.81 (m, 2H, CH_2), 1.99 (m, 4H, CH_2), 3.36 (m, 4H, NCH_2), 7.17 (d, 1H, J=8.30 Hz, naphthalic H′3), 7.25–7.70 (m, 10H, anthralic H2, H3, H4, H5, H6, H7, and H10; naphthalic H′6; phthalic H″3 and H″4), 8.12–8.17 (dd, 2H, J'=4.21 Hz, J''=8.78 Hz, phthalic H″2 and H″5), 8.36 (d, 1H, J=8.55 Hz, H′5), 8.43 (d, 1H, J=8.06 Hz, H′2), 8.52 (d, 1H, J=7.32 Hz, H′5), 8.64 (s, 1H, H9). Mass spectrum m/e: calcd., 601.7; found, 601.8.

6.1.10. 1-(N′-Octyl-1,2,4,5-benzene diimide-N-yl)-8-(4-piperidyl-1,8-naphthalic imidyl)-9,10-dihydro-9,10-(dimethyl carboxyetheno)anthracene (6a)

A solution of **5a** (63 mg, 0.08 mmol) and dimethyl acetylenedicarboxylate (65 mg, 0.46 mmol) in xylene (10 ml) was heated at reflux for 24 h. The resulting dark brown solution was then brought to dryness by removal of solvent under reduced pressure. The residue was purified by preparative TLC using 4% acetone in chloroform as the eluent. This afforded product **6a** (42 mg, 56.8% yield) as an orange–yellow solid. There was also some starting material **5a** (18 mg) recovered. ^{1}H NMR ($CDCl_3$) δ 0.90 (t, 3H, $CH_2(CH_2)_6CH_3$), 1.26–1.38 (m, 10H, $CH_2CH_2(CH_2)_5CH_3$), 1.75 (m, 4H, piperidyl H‴4, and $CH_2CH_2(CH_2)_5CH_3$), 1.90 (m, 4H, piperidyl H‴3 and H‴5), 3.00 (s, 3H, $COOCH_3$), 3.03 (s, 3H, $COOCH_3$), 3.15 (m, 4H, piperidyl H‴2 and H‴6), 3.88 (m, 2H, $CH_2CH_2(CH_2)_5CH_3$), 5.21 (d, 1H, anthralic H10), 5.70 (s, 1H, anthralic H9), 8.01 (s, 2H, pyromellitic H″3 and H″6), 6.74–8.06 (m, 11H, anthralic H2, H3, H4, H5, H6, and H7; naphthalic H′2, H′3, H′5, H′6, and H′7). Mass spectrum m/e: calcd. for $(M+Na)^+$, 948.0; found, 948.8.

6.1.11. 1-(N′-Octyl-1,2,4,5-benzene diimide-N-yl)-5-(4-piperidyl-1,8-naphthalic imidyl)-9,10-dihydro-9,10-(dimethyl carboxyetheno)anthracene (6b)

A solution of **5b** (40 mg, 0.05 mmol) and dimethyl acetylenedicarboxylate (2.0 ml) in xylene (10 ml) was heated at reflux under nitrogen overnight. The resulting dark brown solution was then brought to dryness by removal of solvent under reduced pressure. The residue was purified by preparative TLC using chloroform as the developing solvent. This gave product **6b** (42 mg, 88.9% yield) as a yellow solid. ^{1}H NMR ($CDCl_3$) δ 0.89 (t, 3H, $CH_2(CH_2)_6CH_3$), 1.22–1.35 (m, 10H, $CH_2CH_2(CH_2)_5CH_3$), 1.76 (m, 4H, piperidyl H‴4, and $CH_2CH_2(CH_2)_5CH_3$), 1.94 (m, 4H, piperidyl H‴3 and H‴5), 2.87 (s, 3H, $COOCH_3$), 2.95 (s, 3H, $COOCH_3$), 3.36 (m, 4H, piperidyl H‴2 and H‴6), 3.78 (m, 2H, $CH_2CH_2(CH_2)_5CH_3$), 5.37 (s, 1H, anthralic hydro H10), 5.45 (s, 1H, anthralic hydro H9), 6.81 (d, 1H, J=7.56 Hz, naphthalic H′3), 6.83-7.24 (m, 4H, anthralic H3, H4, H7, and H8), 7.34 (d, 1H, J=6.35 Hz, anthralic H6), 7.43 (d, 1H, J=7.33 Hz, anthralic H2), 7.75 (t, 1H, naphthalic H′6), 8.01 (s, 2H, pyromellitic H″3 and H″6), 8.44 (d, 2H, naphthalic H′2 and H′7), 8.52 (d, 1H, naphthalic H′5). Mass spectrum m/e: calcd. for $(M+Na)^+$, 948.0.0; found, 947.8.

Acknowledgements

This work was supported by the Division of Chemical Sciences, Office of Basic Energy Sciences, United States Department of Energy under contract No. W-31-109-Eng-38.

References

[1] M.R. Wasielewski, Photoinduced Electron Transfer in Supramolecular Models for Artificial Photosynthesis, *Chem. Rev., 92* (1992) 435–461.
[2] D. Gust, T.A. Moore and A.L. Moore, Molecular mimicry of photosynthetic energy and electron transfer, *Acc. Chem. Res., 26* (1993) 198–205.
[3] H. Kurreck and M. Huber, Model reactions for photosynthesis—Photoinduced charge and energy transfer between covalently linked porphyrin and quinone units, *Angew. Chem. Int. Ed. Engl., 34* (1995) 849–866.
[4] J.R. Miller, J.V. Beitz and R.K. Huddleston, Effect of free energy on rates of electron transfer between molecules, *J. Am. Chem. Soc., 106* (1984) 5057–5068.
[5] J.L. Sessler, B. Wang and A. Harriman, Photoinduced energy transfer in associated but noncovalently linked photosynthetic model, *J. Am. Chem. Soc., 117* (1995) 704–714.
[6] J.A. Roberts, J.P. Kirby and D.G. Nocera, Photoinduced electron transfer within a donor–acceptor pair juxtaposed by a salt bridge, *J. Am. Chem. Soc., 117* (1995) 8051–8052.
[7] H. Oevering, J.W. Verhoeven, M.N. Paddon-Row and J.M. Warman, Charge-transfer absorption and emission resulting from long-range through-bond interaction; exploring the relationship between electronic coupling and electron-transfer in bridged donor–acceptor systems, *Tetrahedron, 45* (1989) 4751–4766.
[8] K.W. Penfield, J.R. Miller, M.N. Paddon-Row, E. Cotsaris, M.O. A and N.S. Hush, Optical and thermal electron transfer in rigid difunctional molecules of fixed distance and orientation, *J. Am. Chem. Soc., 109* (1987) 5061–5065.
[9] J.W. Verhoeven, Electron transport via saturated hydrocarbon bridges: exciplex emission from flexible, rigid and semiflexible bichromophores, *Pure Appl. Chem., 62* (1990) 1585–1596.
[10] E.H. Yonemoto, G.B. Saupe, R.H. Schmehl, S.M. Hubig, R.L. Riley, B.L. Iversonh and T.E. Mallouk, Electron-transfer reactions of ruthenium trisbipyridyl-viologen donor-acceptor molecules: comparison of the distance dependence of electron-transfer rates in the normal and marcus inverted regions, *J. Am. Chem. Soc., 116* (1994) 4786–4795.
[11] F.C. DeSchryver, D. Declercq, S. Depaemelaere, E. Hermans, A. Onkelinx, J.W. Verhoeven and J. Gelan, Photophysics of linked donor-acceptor systems: through-space and through-bond interactions, *J. Photochem. Photobiol. A, 82* (1994) 171–179.
[12] S.L. Larson, S.M. Hendrickson, S. Ferrere, D.L. Derr and C.M. Elliott, Energy transfer in rigidly-linked heterodinuclear Ru(II)/Fe(II) polypyridyl complexes: Distance and linkage dependence, *J. Am. Chem. Soc., 117* (1995) 5881–5882.
[13] D. Gosztola, H. Yamada and M.R. Wasielewski, Electric field effects of photogenerated ion pairs on nearby molecules: a model for the carotenoid band shift in photosynthesis, *J. Am. Chem. Soc., 117* (1995) 2041–2048.

[14] C.K. Chang and I. Abdalmudhi, Anthracene pillared cofacial diporphyrin, *J. Org. Chem., 48* (1983) 5388–5390.

[15] M. Sasayama and Y. Naruta, Preparation of a 1,8-anthracene-linked manganese(IV) porphyrin dimer and its reduction with H_2O_2. The O_2 evolution stage by the reduction of the $Mn(IV)_2$ complex is not a rate-determining step in the catalytic disproportionation of H_2O_2, *Chem. Lett.,* (1995) 63–64.

[16] R. Guilard, S. Brandes, A. Tabard, N. Bouhmaida, C. Lecomte, P. Richard and J.-M. Latour, Synthesis, characterization and reactivity toward dioxygen of copper manganese cofacial porphyrins. Crystal and molecular structures of a heterobimetallic biphenylene-pillared cofacial diporphyrin, *J. Am. Chem. Soc., 116* (1994) 10202–10211.

[17] A. Osuka, T. Nagata, F. Kobayashi, R.P. Zhang, K. Maruyama, N. Mataga, T. Asahi, T. Ohno and K. Nozaki, Long-lived charge separated states from distance fixed triads consisting of zinc porphyrin, free-base porphyrin, and pyromellitimide, *Chem. Phys. Lett., 199* (1992) 302–308.

[18] S.R. Greenfield, W.A. Svec, D. Gosztola and M.R. Wasielewski, Multistep photochemical charge separation in rod-like molecules based on aromatic imides and diimides, *J. Am. Chem. Soc., 118* (1996) 6767–6777.

[19] A. Weller, Photoinduced electron transfer in solution: exiplex and radical ion pair formation free enthalpies and their solvent dependence, *Z. Phys. Chem., 133* (1982) 93–98.

[20] J.M. Warman, K.J. Smit, S.A. Jonker, J.W. Verhoeven, H. Oevering, J. Kroon, M.N. Paddon-Row and A.M. Oliver, Intramolecular charge separation and recombination in non-polar environments via lon-distance electron transfer through saturated hydrocarbon barriers, *Chem. Phys., 170* (1993) 359–380.

[21] I.R. Gould, D. Noukakis, L. Gomez-Jahn, R.H. Young, J.L. Goodman and S. Farid, Radiative and nonradiative electron transfer in contact radical-ion pairs, *Chem. Phys., 176* (1993) 439–456.

[22] R.A. Marcus, On the theory of electron-transfer reactions. VI. Unified treatment for homogeneous and electrode reactions, *J. Chem. Phys., 43* (1965) 679–701.

[23] G.L. Closs and J.R. Miller, Intramolecular long-distance electron transfer in organic molecules, *Science, 240* (1988) 440–447.

[24] Hypercube, Waterloo, Ont., Canada.

[25] A.P. deSilva, H.Q.N. Gunaratne, J.-L. Habib-Jiwan, C.P. McCoy, T.E. Rice and J.-P. Soumillion, New fluorescent model compounds for the study of photoinduced electron transfer: The influence of a molecular electric field in the excited state., *Angew. Chem. Int. Ed. Engl., 34* (1995) 1728–1731.

[26] J.A. Riddick, W.B. Bunger and T.K. Sakano, *Organic Solvents: Physical Properties and Methods of Purification,* Wiley, New York, 1986.

[27] J.J. Hopfield, Electron transfer between biological molecules by thermally activated tunneling, *Proc. Natl. Acad. Sci. USA, 71* (1974) 3640–3644.

[28] J. Jortner, Temperature dependent activation energy for electron transfer between biological molecules, *J. Chem. Phys., 64* (1976) 4860–4867.

[29] R.A. Marcus, Nonadiabatic processes involving quantum-like and classical-like coordinates with applications to nonadiabatic electron transfers, *J. Chem. Phys., 81* (1984) 4494–4500.

[30] Y. Sakata, H. Tsue, M.P. O'Neil, G.P. Wiederrecht and M.R. Wasielewski, Effect of donor–acceptor orientation on ultrafast photoinduced electron transfer and dark charge recombination in porphyrin-quinone molecules, *J. Am. Chem. Soc, 116* (1994) 6904–6909.

[31] T. Shida, *Electronic Absorption Spectra of Radical Ions,* Elsevier, Amsterdam, 1988.

[32] J.N. Miller, *Standards in Fluorescence Spectrometry,* Chapman and Hall, London, 1981.

[33] H.A. Frank, A. Cua, A. Young, D. Gosztola and M.R. Wasielewski, Photophysics of the carotenoids associated with the xanthophyll cycle in photosynthesis, *Photosynthesis Res., 41* (1993) 389–395.

[34] J.L. Sessler, T.D. Mody, D.A. Ford and V. Lynch, A nonaromatic expanded porphyrin derived from anthracene—A macrocycle which unexnnpectedly binds anions, *Angew. Chem. Int. Ed. Engl., 31* (1992) 452–453.

[35] H.O. House, J.T. Holt and D. VanDerveer, Unsymmetrically substituted 2,7-dimethyl-1,8-diarylanthracenes, *J. Or. Chem., 58* (1972) 7516–7523.